Alma Mater Studiorum Università di Bologna
Archivio istituzionale della ricerca

Assessing aquitard integrity in a complex aquifer – aquitard system contaminated by chlorinated hydrocarbons

(Article begins on next page)

04 September 2024

1   **Assessing aquitard integrity in a complex aquifer – aquitard system contaminated by chlorinated**

2   **hydrocarbons**

3

4   **Maria Filippini[a], Beth L. Parker[b], Enrico Dinelli[a], Philipp Wanner[b, c], Steven W. Chapman[b], Alessandro**

5   **Gargini[a]**

6

7   [a]Department of Biological, Geological and Environmental Sciences, Alma Mater Studiorum University of

8   Bologna, via Zamboni 67, 40126 Bologna, Italy

9   [b]G360 Institute for Groundwater Research, College of Engineering & Physical Sciences, University of

10   Guelph, 50 Stone Road East, Guelph, Ontario, Canada N1G 2W1

11   [c]Institute of Geological Sciences – RWI, Baltzerstrasse 1 & 3, CH-3012 Bern, Switzerland

12

13   **Abstract**

14   This study investigates for the first time the integrity of multiple stacked aquitards with different degrees of

15   reactivity to contaminant degradation. Aquitard integrity was assessed in a contaminated, multi-layered,

16   alluvial aquifer-aquitard system (Ferrara, northern Italy). The system was contaminated by mixed organic

17   contaminants of industrial origin (mostly chlorinated ethenes) that were illegally disposed in an urban

18   dump four to five decades ago. High spatial resolution profiles of hydraulic head, geochemistry and

19   chlorinated hydrocarbon concentrations were determined through the multi-layered system via discrete

20   interval sampling of continuous cores and multilevel groundwater sampling, at three locations aligned

21   along a transect adjacent to the buried waste to a maximum depth of 53 meters below the water table.

22   The profiles revealed that the two shallow aquitards had low integrity with respect to impeding downward

23   migration of dense non-aqueous phase liquid (DNAPL), and provided little protection to the underlying

24   aquifers against DNAPL contamination due to preferential pathways through imperceptible fractures

25   and/or permeable micro-beds. However, both aquitards inhibited downward DNAPL migration to some

26   extent due to DNAPL retention along its flow paths and accumulation at lower permeability interfaces, with

27 decreasing peak concentrations at the top of successively deeper aquitard units. Moreover, both aquitards

28 enhanced contaminant biodegradation due to the occurrence of organic rich sub-layers, influencing the

29 contaminant plume composition, mobility and fate in the underlying and overlying aquifers.

30 The deepest aquitard showed evidence of DNAPL accumulation at the top and slow diffusion-dominated

31 transport consistent with 40 years of transport, suggesting higher integrity compared to the two shallower

32 aquitards. However, the occurrence of micro-fractures and/or discontinuities in the aquitard upgradient

33 under the dump (source) is the most likely explanation for contamination of the deepest aquifer. Analytical

34 1-D simulations of the diffusion profiles in the deepest aquitard revealed that DNAPL contamination down

35 to the top of this aquitard occurred with minimal delay after DNAPL waste disposal began.

36 The results highlight the necessity of high-resolution vertical profiling for assessing the presence of

37 imperceptible features relevant to DNAPL migration and integrity of individual aquitards affecting organic

38 contaminant source zone mass and phase distributions over decades.

39

40 KEY WORDS: aquitard integrity, chlorinated ethenes, DNAPL, source zone age and evolution, diffusion mass

41 transfer, fluvial sediments

42

43 **1 Introduction**

44 The integrity of an aquitard refers to its capability to protect an underlying aquifer against contamination

45 (Cherry et al. 2006, Parker et al. 2004). Until a few decades ago it was assumed that aquitards generally

46 prevent contamination of underlying confined aquifers from surface contamination sources (e.g. Ponzini et

47 al. 1989, U.S. EPA 1987). However, contaminant occurrences in confined aquifers were observed since the

48 1990's, often involving chlorinated hydrocarbons as dense non-aqueous phase liquids (DNAPL) in the

49 source zones (e.g. PPG Industries 1995, Chapuis 2013, Pedretti et al. 2013, Fjordbøge et al. 2017). This

50 contradicts the assumption that low permeability sediments with hydraulic conductivities less than 10^{-7}

51 cm/s (based on USEPA guidance for compacted clay landfill liners, e.g. Green et al. 1981) generally prevent

52 the migration of contaminants into underlying aquifers. Research at industrial waste disposal sites in the

53   1990's suggested that deep DNAPL migration can be attributed to pre-existing fractures in natural clay-rich

54   sediments that are imperceptible in bulk hydraulic conductivity testing (Cherry et al. 2006, Wills et al.

55   1992).

56   Mathematical modeling and laboratory studies (Jørgensen et al. 1998, O'Hara et al. 2000, Kueper and

57   McWhorter 1991, McWhorter and Kueper 1996) demonstrated that DNAPLs have an exceptional

58   propensity to enter and migrate through very small fractures, even those with hydraulic apertures smaller

59   than 10 μm. These observations were confirmed by several field studies. PPG Industries (1995) reported

60   the migration of tetrachlorethylene (PCE) and trichlorethylene (TCE) DNAPLs through a 50 m thick alluvial

61   clay aquitard to the underlying aquifer at a chemical manufacturing facility, due to root holes and fractures

62   acting as preferential pathways for DNAPL migration. Chapuis (2013) observed high concentrations of

63   chlorinated hydrocarbons in a confined aquifer overlain by a glacial till aquitard, where DNAPL migration

64   through micro-fractures was the most likely explanation. Fjordbøge et al. (2017) characterized a clay till

65   aquitard underlying a PCE and TCE DNAPL source zone, where vertical migration of DNAPL occurred

66   through fractures in a shallow oxidized zone and to a lesser extent through a less fractured reduced zone,

67   reaching the underlying confined limestone aquifer. Beside fractures, unlithifed clay-rich aquitards in

68   alluvial settings often enclose thin sand intercalations that can create a stair-step pattern of preferential

69   flow paths for DNAPL flow (e.g. Morrison et al. 1998, Parker 1996). Pedretti et al. (2013) observed

70   lithologic heterogeneities in a shallow clay aquitard while investigating the distribution of chlorinated

71   hydrocarbon contamination (mainly PCE and TCE) at the regional scale in an alluvial multi aquifer-aquitard

72   system, where contaminants breached the clay aquitard at several sites in the region, reaching the

73   underlying confined aquifer. The literature also reports some aquitards capable of preventing DNAPL

74   penetration or allow only partial migration. Morrison et al. (1998) reported partial PCE DNAPL penetration

75   in a thin surficial clayey aquitard at a site where DNAPL was released under controlled conditions. Vertical

76   microfractures allowed DNAPL migration through an upper part, whereas the lower part provided

77   resistance to DNAPL flow. Parker et al. (2004) showed TCE DNAPL accumulation at the bottom of a sandy

78   aquifer overlying a thick aquitard at an industrial property. Diffusion profiles of dissolved contaminants

79   were observed in the upper part of the aquitard, but with no evidence of DNAPL penetration attributed to

80   lack of fractures given the plasticity of this lacustrine sediment and lack of post-deposition exposure.

81   Adamson et al. (2015a) and Adamson et al. (2015b) advanced the use of diffusion transport contaminant

82   concentration profiles in low permeability clay-rich sediments as a means to assess contaminant source

83   zone history after Parker et al. (1994) and Parker et al. (2004). The source history model proposed by

84   Adamson et al. (2015b) was demonstrated at two industrial sites with chlorinated ethenes and ethanes,

85   showing that after decades most of the contaminant mass occurred in the low permeability aquitard layers

86   due to diffusion enhanced by sorption, with high aquitard integrity with respect to DNAPL penetration, but

87   also how diffusive mass transfer alters the location and phase of contamination.

88   Notwithstanding the existing literature, the parameters that control the integrity of clayey aquitards are

89   not yet clear and often appear to be strongly site-specific requiring careful investigation methods including

90   collection and sampling of minimally disturbed continuous cores. Thus, there is a need for improving the

91   scientific knowledge with respect to different DNAPL source conditions and geologic settings for assessing

92   aquitard integrity. The objective of this paper is to evaluate the integrity of distinct silt and clay-rich, non-

93   indurated (unlithified) aquitards of fluvial origin with different degrees of reactivity to contaminant

94   biodegradation. To the best of our knowledge, the assessment of the integrity of multiple stacked reactive

95   aquitards was never reported in the literature. For this purpose, a site was selected where a 60-m thick

96   multi-layered aquifer-aquitard system of alluvial origin was contaminated by chlorinated aliphatic

97   hydrocarbons, predominantly with chloroethenes, originating from a known mixed DNAPL source. High-

98   resolution hydraulic head, geochemistry and chlorinated hydrocarbon concentration profiles were

99   determined using continuous cores along a transverse cross-section (i.e. transect) adjacent to the

100   contamination source. The investigated multi-layered aquifer-aquitard configuration is representative of

101   many other alluvial systems (e.g. Blum and Törnqvist 2000) so the insights as well as the methods applied

102   are useful for assessment of non-indurated aquitard integrity at other sites.

103

104   **2 Site Description**

105   The selected "Caretti site" is located 1 km east of the historical center of Ferrara in the eastern sector of the

106   Padana plain, about 4 km south of the Po river and covers an area of about 1 km^2 (Fig. 1). The

107   hydrostratigraphy exhibits an alternation of fine to coarse grained sands of higher hydraulic conductivity

108   (aquifers) and silty–clayey layers of lower hydraulic conductivity (aquitards), to a depth of around 200 m

109   below ground surface (m bgs) (Molinari et al. 2007). Three aquifers are in the upper 60 m bgs indicated as

110   A0, Upper A1, and Lower A1 (Regione Emilia-Romagna and ENI-AGIP 1998), whereby each of them is

111   overlain by a non-indurated aquitard named after the underlying aquifer: Q0, Upper Q1 and Lower Q1 (Fig.

112   2). The A0 aquifer consists of scattered sandy lenses intermingled with fine-grained deposits (Amorosi and

113   Colalongo 2005); the Upper A1 aquifer is characterized by low spatial continuity (i.e. low amalgamation

114   between sandy lenses, that form sandy bodies extended for 10 to 100 m^2), whereas the Lower A1 aquifer is

115   a regionally extensive sandy body (on the scale of 10000 m^2). The main groundwater flow direction at the

116   Caretti site is NNE in the A0 aquifer, NW in the Upper A1 aquifer and E in the Lower A1 (Nijenhuis et al,

117   2013; Filippini et al. 2016). Two main sources contribute to the recharge of the multi-aquifer system: The

118   Po river (lateral recharge) and the local rainfall (vertical recharge) (Rapti-Caputo and Martinelli 2009). The

119   averaged contribution of vertical recharge decreases from 75% in the A0 down to 26% in the Lower A1

120   whereas the lateral recharge increases with increasing aquifer depth from 25% in the A0 up to 74% in the

121   Lower A1 (Filippini et al. 2015). In the Ferrara region, the confined Lower A1 aquifer is exploited at several

122   locations for irrigation or drinking water supply and the overlying Lower Q1 aquitard is considered capable

123   to protect the quality of this aquifer, as reported in several technical documents (not published). Previous

124   investigations at the Caretti site (Gargini et al. 2011) revealed that the aquifers A0 and Upper A1 are

125   contaminated by chlorinated hydrocarbons, originating from urban waste and chlorinated pitches

126   containing a mixture of chlorinated ethenes and ethanes that were deposited primarily as DNAPL in a clay

127   pit (known as Southern Dump) between the late 1950s and 1970s (Fig. 1). Groundwater contamination by

128   chlorinated hydrocarbons was first detected in 2000 by the local environmental authority, during an

129   investigation for the development of a new residential area. Two chlorinated hydrocarbon plumes were

130   identified in the A0 and Upper A1 aquifers that have migrated about 500 m down-gradient of the Southern

131   Dump (Fig. 1). The plume in the A0 aquifer consists primarily of chloroethenes (PCE; TCE; 1,1-

132   dichloroethene – 11DCE; cis-1,2-dichloroethene – cDCE; trans-1,2-dichloroethene – tDCE; vinyl chloride –

133   VC), and secondarily of chloroethanes (1,1,1,2-tetrachloroethane – 1112TeCA; 1,1,2,2-tetrachloroethane –

134   1122TeCA; 1,1,2-trichloroethane – 112TCA; 1,2-dichloroethane – 12DCA) and chloromethanes (carbon

135   tetrachloride – CT; chloroform – CF; dichloromethane – DCM). Only chloroethenes (PCE, TCE, 11DCE, cDCE,

136   tDCE) and a few chloroethanes and chloromethanes (1122TeCA, 112TCA, CF, DCM) were detected in the

137   plume of the Upper A1 aquifer. The Lower A1 aquifer is considered uncontaminated based on separate

138   characterization efforts by the local authorities.

139

140   **3 Materials and Methods**

141   **3.1 Types of data collected**

142   Stratigraphic, hydraulic head and chemical data were collected along a 60 m wide x 60 m deep cross-

143   section (i.e. transect) located at the northern end of the Southern Dump perpendicular to the groundwater

144   flow direction of the A0 aquifer. The transect consists of two deep profiles (60 m bgs: MC1-2 and MC4-5) at

145   both ends and one shallower profile (30 m bgs: MC3) in the center (Fig. 2), whereby the horizontal distance

146   between the three profiles is 30 m. Data collection and analysis are described in the following sections and

147   further in the Supplementary Material (SM).

148

149   **3.2 Continuous coring and core subsampling**

150   Continuous cores were collected from the three locations in July 2013 using a wireline coring system with

151   triple tube core barrel that provided consistent, high core recovery of 95-98%. For the two deep profiles

152   (MC1-2 and MC4-5) cores were collected at slightly different locations (4-5 m apart) for the shallower (0-30

153   m bgs) and the deeper interval (28 – 60 m bgs) (Fig. 2). Before collecting cores from the deeper interval, the

154   upper 28 m of the borehole was sealed with permanent casing to avoid cross-contamination of the deepest

155   aquifer (Lower A1). Upon retrieval at ground surface, the cores were split longitudinally; one half was used

156   for detailed lithostratigraphic descriptive logging and Pocket penetrometer tests (Eijkelkamp Pocket

157 Penetrometer – Model 06.03) to evaluate sediment consistency, while the other half was used for

158 collection of large sediment samples (~250 g each). The sediment samples were collected at a one meter

159 spacing at locations MC1-2 and MC3 for measurement of grain size distributions in the sandy and silty clay-

160 rich layers. At the MC4-5 location, the other half of the cores was subsampled for measurement of

161 chlorinated hydrocarbon concentrations and for determination of porosity and organic carbon content. The

162 MC4-5 location was selected to perform the sediment core subsampling as it was expected to be the most

163 contaminated profile based on previous site characterization (Gargini et al., 2011; Nijenhuis et al., 2013).

164 Stratigraphic information from the cores was complemented by piezocone penetration tests (CPTU) to 30

165 m depth performed by the municipality of Ferrara 50 m southeastward from the transect (Fig. 1).

166 Core subsampling was conducted following the procedure described by Wanner et al. (2016), Adamson et

167 al. (2015a), Parker et al. (2004) and Parker et al. (2003), targeting a vertical spacing along the core axis of

168 about 10 cm. Three subsamples were collected at each depth (297 sampling depths in total), one for

169 chlorinated hydrocarbon concentration analyses, one for sediment properties (total porosity - ϕ, and

170 organic carbon fraction - f_{oc}), and a third for screening for the presence of DNAPL phase using a

171 hydrophobic dye (Oil-Red-O).

172

173 **3.3 Multilevel systems for hydraulic head and groundwater chemistry profiles**

174 After coring, groundwater multilevel monitoring systems were installed in the five boreholes along the

175 transect (Fig 2). Among the commercially available multilevel systems, the Solinst® CMT System (Einarson

176 2006) was selected, because: 1) it is suitable for unconsolidated sediment settings (Einarson and Cherry

177 2002) and 2) it allows selection of screen position and lengths in the field based on borehole-specific

178 lithology distributions from core logging. Each of the five CMT systems was equipped with 7 screens at

179 discrete depths targeting both aquifers and aquitards and avoiding cross-connection across visually distinct

180 permeability zones (Fig. 2).

181 Groundwater from the CMTs was sampled in November 2013 using dedicated 6 mm OD Teflon tubing and a

182 peristaltic pump (Model 410 Peristaltic Pump, Solinst[®]) to perform cation, anion and chlorinated

183 hydrocarbon concentration analyses.

184 Hydraulic heads were manually monitored in the CMTs twice a week between September 9, 2013 and July

185 28' 2014 (321 days) using a 4 mm diameter water level meter (Model 102 narrow diameter cable water

186 level meter, Solinst[®]).

187

188 **3.4 Lab analyses of sediment and groundwater samples**

189 Chlorinated hydrocarbon concentration analyses on core subsamples was performed at the University of

190 Guelph, ON, Canada. The contaminants were extracted from the sediment subsamples as described by

191 Dincutoiu et al. (2003). The analytical technique provides the total chlorinated hydrocarbon analyte mass

192 per mass of wet sediment (C_t) and does not distinguish between the aqueous, sorbed and NAPL phases.

193 Assuming DNAPL-free conditions, the pore water concentration (C_w) and sorbed mass concentration (C_s) in

194 the sediment subsamples can be estimated assuming equilibrium partitioning between dissolved and

195 sorbed phases (e.g. Parker et al. 2004, Adamson et al. 2015a). In addition to direct field screening tests with

196 dye, occurrence of pure phase DNAPL in the sediment samples was verified by comparing the estimated C_w

197 of each compound derived from C_t measurements in sediment samples with their effective solubility based

198 on an estimated analyte mole fraction (provided in SM).

199 Anion concentrations in groundwater were analyzed at the University of Bologna, Italy, by ion exchange

200 high performance liquid chromatography using a Metrohm 883 Basic IC Plus chromatograph. Cations were

201 analyzed in the same lab by Flame Atomic Absorption Spectrometry using a Perkin Elmer AA100

202 spectrometer. Chlorinated hydrocarbon concentrations in groundwater samples were analyzed by a

203 private certified laboratory (Chelab S.r.l., Treviso, Italy), using the analytical methods EPA 5030 C (U.S. EPA

204 2003) and EPA 8260 C (U.S. EPA 2006).

205

206 **3.5 Analytical modeling of diffusive transport in aquitard Lower Q1**

207 The aim of the analytical modeling was to estimate the time of contaminant arrival based on fitting of the

208 concentration with distance profiles measured in the Lower Q1 aquitard with field and/or literature derived

209 parameters for the sediment and solute. The PCE and TCE profiles appeared to be diffusion controlled and

210 PCE and TCE transport in the Lower Q1 aquitard was simulated using a 1D analytical solution of Fick's

211 Second Law assuming linear, instantaneous sorption (e.g. Parker et al. 2004, Parker 1996, Narasimhan

212 2004) for a homogeneous, semi-infinite porous medium (e.g. Carslaw and Jaeger 1959):

213 $C_w = C_0 \, erfc \, (z/(2(tD_e/R)^{1/2})$ (1)

214 where C_w is the chlorinated hydrocarbon pore water concentration (mg/L), C_o is the concentration at the

215 Upper A1-Lower Q1 interface acting as boundary concentration, R is the retardation factor due to sorption

216 (eq. S9, in th SM), D_e is the effective molecular diffusion coefficient in the porous medium (cm^2/s), z is the

217 vertical depth (cm), with z =0 at the aquitard interface, and t is time (s). Biodegradation of parent

218 compounds in the Lower Q1 aquitard was assumed to be minor and not included in the simulations, as the

219 chlorinated hydrocarbon concentration analyses did not show occurrence of the dechorination product VC,

220 and relatively low concentrations of cDCE (max 0.6 mg/L) compared to much higher concentrations of the

221 parent compounds PCE and TCE (max 37 and 10 mg/L, respectively). In the case of PCE, a constant

222 concentration was fixed at the model interface based on the characteristic shape of the profile with

223 concentrations declining with distance into the aquitard suggesting relatively steady concentrations at the

224 interface, and the diffusion time was used as a fitting parameter by varying it until a minimal deviation

225 between measured and modelled concentrations was obtained. In contrast the TCE profile showed a profile

226 shape consistent with a declining concentration at the interface, and thus a temporal evolution (step-

227 decline) of the TCE concentration at the interface was evaluated. This decline was taken into account by

228 superimposing analytical solutions to simulate a two-step concentration at the interface with C_w calculated

229 for both steps using eq. S7 (in the SM). In the first step, a high TCE concentration representative of an

230 earlier contamination stage was fixed at the model interface applying the entire diffusion time obtained

231 from the PCE modeling. In the second step, a lower TCE concentration was assigned at the interface over a

232 shorter time period to simulate a second stage when the boundary concentration was clearly lower, and by

233 applying the concept of superposition, these results were subtracted from results of the first step to obtain

234 the combined profile. The diffusion time of the second step and the interface TCE concentrations of both

235 steps were varied until reaching minimal deviation between measured and modeled concentrations.

236 Deviation between measured (m) and modeled (M) concentrations was quantified using the Nash-Sutcliffe

237 model efficiency coefficient (NSE; Nash and Sutcliffe 1970, Legates and McCabe Jr 1999):

238 $NSE = 1 - \sum_{n=1}^{i} (m_i - M_i)^2 / \sum_{n=1}^{i} (m_i - m_m)^2$ (2)

239 where m_m is the measured mean. NSE ranges from minus infinity to 1 with higher values indicating better

240 fit.

241 Adamson et al. (2015b) recently provided a source history model for estimating interface concentration

242 history based on measured low-K zone profiles, which was applied as a verification for the analytically

243 simulated profiles, and for refining the concentration history at the interface for the TCE profile. The

244 primary difference for the fits using the source history model is that the total mass concentrations (C_t) are

245 used as primary input whereas the porewater concentration (C_w) are estimated by the model applying

246 average parameter values for bulk density, porosity ϕ, and estimated R factor. The source history

247 simulation results are provided in the SM.

248

249 **4. Results and discussion**

250   **4.1 Contaminant distributions as evidence for aquitard integrity**

251 The thickness of aquitard Q0 at the site is clearly altered due to past excavation for waste disposal. The

252 waste material likely reaches a thickness equal to or higher than the thickness of Q0 in the area of the

253 transect (e.g. in the MC3 profile only 1 m of fine-grained deposits of the Q0 aquitard separate the wastes

254 from the A0 aquifer; Fig. 3). Thus, the integrity of the aquitard Q0 is difficult to assess as the contaminants

255 may have reached the underlying A0 aquifer either due to poor integrity of the Q0 or because the waste

256 dumps penetrated the Q0 due to excavations and contacted the top of the A0 directly. Peaks of

257 chloroethene concentrations were detected into the Q0 aquitard from sediment samples along core MC4-5

258 (mostly cDCE and VC with estimated pore water concentrations, C_w, up to 197 and 16 µg/L, respectively)

259   that suggest strong contaminant retention and degradation in the aquitard layer (Fig. 4). Occurrence of

260   chloroethenes in the Q0 is also confirmed by groundwater concentrations (GW) along profiles MC4-5 and

261   MC3. The absence of contaminants into this aquitard along profile MC1-2 is more likely justified by the

262   absence of residual waste above the profile (Fig. 3) rather than locally high Q0 aquitard integrity, since the

263   profile is positioned at the edge of or beyond the source zone.

264   The cumulative mass distribution per unit area of total VOCs, chloroethenes, chloroethanes and

265   chloromethanes along the MC4-5 profile suggests accumulation contaminants at the interface between

266   aquifer A0 and aquitard Upper Q1 (especially PCE, cDCE, 1122TeCA and 112TCA, with peak C_w of 54, 141, 86

267   and 23 µg/L, respectively) and at the interface between aquifer Upper A1 and aquitard Lower Q1 (mostly

268   PCE and TCE, with max C_w of 37 and 10 µg/L, respectively) in a manner consistent with DNAPL migration

269   and preferential accumulation at those interfaces where capillary pressures were insufficient to invade

270   sediments with different and smaller pore geometry (Fig. 5). The major mass accumulation zone occurs at

271   the top of the Upper Q1 aquitard showing strong resistance of DNAPL penetration (i.e. resistance to vertical

272   flow) and enhanced lateral DNAPL migration in this system, as evidenced by the sudden occurrence of the

273   chloroethanes, and their absence above this depth. This mass accumulation also corresponds to organic-

274   rich sublayers in the top meter of the Upper Q1 aquitard (max f_{oc} of 2.6% at 9.5 m bgs; see Fig. 3) where the

275   organic sediment facilitates contaminant retention by sorption. The same organic-rich sublayers provide a

276   favorable environment for reductive dechlorination. Filippini et al. (2016) observed reductive

277   dechlorination of chloroethenes PCE and TCE and accumulation of by-products (mainly cDCE and VC) during

278   contaminant retention and migration within these fine organic-rich sediments. By analogy, chlorinated

279   ethanes 112TCA, 12DCA, and methanes DCM, CM that occur exclusively in the shallowest 10-12 m of the

280   profile are likely by-products from dechlorination of higher chlorinated compounds (e.g. 1112TeCA,

281   1122TeCA and CF).

282   Despite the high resistance to DNAPL penetration inferred for the Upper Q1 aquitard, the cumulative mass

283   profiles strongly support some DNAPL invasion through this aquitard given the contamination throughout

284   the underlying Upper A1 aquifer down to the top of Lower Q1, where the second largest chloroethene

285   mass accumulation was registered. The low contaminant concentrations in the aquifer Upper A1

286   (interposed between the two contaminated aquitards Upper and Lower Q1) at the time of this investigation

287   are explainable due to the active groundwater flow in the aquifer over the last decades and much lower

288   sorption in the sandy sediments compared to fine-grained organic-rich sediments of the underlying and

289   overlying aquitards. Thus, the present day contaminant distributions appear strongly affected by an earlier

290   contamination stage when DNAPL was migrating preferentially downward and laterally along lower K_v

291   aquitard interfaces. Even though field tests with dye provided negative results along the whole profile, the

292   occurrence of pure phase DNAPL could be inferred in at least one sample within the A0 aquifer where

293   estimated PCE pore water concentration most likely exceeded effective solubility limits (see SM). Few other

294   shallow samples (i.e. from Q0 aquitard, A0 aquifer, and Upper Q1 aquitard) showed pore water

295   concentration possibly close to effective solubility for some compounds. This suggests little remaining and

296   highly residualized DNAPL at the time of investigation, but most likely much more mobile DNAPL nearer the

297   time of disposal.

298   The contaminant profiles from MC4-5 cores show evidence of diffusion dominated transport (i.e.

299   characteristic diffusion profiles) at the top of the lower Q1 aquitard with rapid decrease of concentration

300   below the aquifer-aquitard interface (see Fig. 8), suggesting good aquitard integrity preventing deeper

301   DNAPL penetration into and below this zone. However, the aquitard did not prevent migration of some

302   contaminants into the lower A1 aquifer (PCE and TCE concentrations up to 3 mg/L, much lower than in the

303   overlying aquitard), showing evidence of some DNAPL migration pathways to these depths, which might

304   come from breaches in this aquitard upgradient from the core location with horizontal migration by

305   groundwater flow in the Lower A1. Consideration was given to possible cross-contaminant due to drag-

306   down of much higher concentrations and presence of DNAPL shallower in the profile. However, the field

307   methods involved significant steps to reduce this situation, using a separate borehole with a blank casing

308   through the shallower zone for the deep coring locations. This makes the cross-connection explanation

309   unlikely with the more likely scenario that preferential contaminant pathways must have existed at an early

310   stage, when mobile DNAPLs were present. The propensity for deep migration pathways no longer exists

311 once the mobile DNAPL phase dissolves away to the point where the driving force diminishes, which is the

312 condition expected at the drilling locations, but maybe not internal to the dump area. Contaminant

313 concentration profiles at the top of the lower Q1 aquitard are discussed in Section 4.3 providing insights on

314 source history.

315

316   **4.2 Hydraulic head and hydrochemistry profiles as complementary evidence**

317 The strongest vertical hydraulic head variations (Δh_v) of about 0.1 m with depth are localized within the

318 Upper Q1 and Lower Q1 aquitards (Fig. 6). A similar variation is observed in the aquitard below the Lower

319 A1 aquifer, which is beyond the zone of relevance of this paper, but confirms repeated occurrence of head

320 losses in all aquitards. The vertical gradient variability along the thickness of an aquitard layer is caused by

321 heterogeneity of the hydraulic conductivity in the vertical direction (K_v), with steeper gradient in sub-layers

322 of lower K_v (Cherry et al. 2006).

323 From a stratigraphic viewpoint, the main Δh_v in the Upper Q1 aquitard occur inside the organic-rich layer

324 from 8 to 11 m bgs, suggesting this is a sub-layer of lower vertical hydraulic conductivity able to reduce

325 groundwater and DNAPL flow between the aquifers A0 and Upper A1. The vertical distribution of field

326 parameters and ion concentrations shows decreasing trends (increasing in the case of pH) from aquifer A0

327 to aquifer Upper A1 suggesting vertical migration down to the Upper A1 aquifer of dissolved components

328 originating from dump leachate and redox influences by the presence of high VOC concentrations (Fig. 7).

329 An exception was observed for potassium (K) and fluoride (F) where concentrations drop close to zero

330 below the Upper Q1 aquitard, possibly due to adsorption onto clay minerals, oxides and/or hydroxides

331 (Pickering 1985, Mitra and Prakash 1956) which are abundant in the Ferrara aquitards (Amorosi et al.

332 2002). Based on these observations, the Upper Q1 appears to be an ineffective barrier against the vertical

333 migration of dissolved ions and especially ineffective barrier to DNAPL. Otherwise, if the A0 and Upper A1

334 aquifer were effectively insulated by the Upper Q1 aquitard, a change in the vertical trends would have

335 been observed between the two aquifers since they are recharged by different sources (Filippini et al.

336 2015) and have different hydrochemistry at the regional scale (Molinari et al. 2007). The low integrity of the

337 Upper Q1 aquitard is likely due to the occurrence of imperceptible fractures and coarse-grained sub-layers

338 of higher K_v that facilitate vertical groundwater exchanges between the over- and underlying A0 and Upper

339 A1 aquifers. The higher ion concentration observed in this aquitard and in the overlying and underlying

340 aquifers along MC4-5 and MC3 profiles in comparison to MC1-2 is explained considering that residual waste

341 only remained at the top of the first two profiles (Fig. 3). An exception is SO_4, which shows the highest

342 concentration in profile MC1-2, while in the more contaminated MC4-5 and MC3 profiles this had likely

343 been depleted as an electron acceptor for reductive biotransformation of chlorinated compounds (Ndon et

344 al. 2000).

345 The lithostratigraphic features of the Lower Q1 aquitard (uniform grain-size, high clay content of 40%, no

346 visual evidence of fracturing) suggest absence of preferential pathways for contaminant migration and

347 thus, a higher degree of integrity compared to the shallower aquitard units. Hydraulic heads in the Lower

348 Q1 shows the occurrence of a sub-layer of low vertical hydraulic conductivity (main Δh_v) localized in the

349 zone of a markedly clayey section from 28 to 30.5 m bgs, characterized by "hard consistency" from pocket

350 penetrometer tests (see Fig. 3). Such layer is expected to provide an effective insulation between the

351 overlying Upper A1 and underlying Lower A1 aquifers. Despite the absence of visible fractures in the

352 aquitard at the core scale, the pore pressure trend (u; kPa) obtained from a CPTU performed 50 m

353 southeastward from the transect shows a sudden decrease of u at the same depth of the main Δh_v in the

354 Lower Q1 aquitard (Fig. 6), indicating an over-consolidation of the layer (Chen and Mayne 1996, Mayne et

355 al. 1990, Amorosi and Marchi 1999) and a consequent prone-to-fracturing behavior ("fragility") with

356 probable occurrence of micro-fractures. Such micro-fractures represent an ideal preferential pathway for

357 the migration of small amounts of DNAPL thought the protective clayey layer of the Lower Q1 aquitard. In

358 the context of the southeastern Po river plain, a high consolidation of clays with consequential micro-

359 fracturing is likely attributed to cohesive sediment desiccation during the prolonged phase of subaerial

360 exposure that characterized the area during the last glacial maximum and the first stages of transgression

361 (Amorosi and Marchi 1999, Rizzini 1974). The typical occurrence of fractures and DNAPL migration

362   pathways in natural clay-rich aquitards was also reported by Morrison et al. (1998) and Cherry et al. (2006)

363   especially in clayey aquitards thinner than 15 meters, of fluvial origin and overconsolidated.

364   Hydrochemistry further distinguishes the lower Q1 aquitard conditions compared to the shallower system.

365   Field parameters and ion concentrations show sharp changes of vertical trends below the Lower Q1

366   aquitard suggesting that the Upper and Lower A1 aquifers have dissimilar hydrochemistry with the Lower

367   Q1 aquitard reducing fluxes between the two aquifers (Fig. 7). In particular, the lowest ion concentrations

368   of the entire profiles were observed at the top of the Lower A1 aquifer, suggesting no or much lower

369   influence from the surficial contaminant inputs compared to the two shallower aquifers. This observation

370   confirms that the propensity for deep migration pathways through the deeper aquitard is only effective in

371   the presence of mobile DNAPL phase but not for dissolved components.

372

373   **4.3 Lower Q1 aquitard integrity from diffusion transport**

374   The contaminant distributions of PCE and TCE at the top of the lower Q1 aquitard show concentration

375   profiles characteristic of transient diffusive transport (Fig. 8). The opportunity was taken to use these

376   profiles for assessing the time of first contaminant arrival at the Lower Q1 aquitard. To this aim, the PCE

377   and TCE profiles were reproduced using a mathematical model for 1-D diffusive transport with linear,

378   instantaneous sorption (described in Section 3.5). The shape of the PCE profile shows the peak

379   concentration at the aquifer-aquitard interface with PCE boundary concentration of 37 mg/L, not far from

380   the lower limit of estimated effective solubility (i.e. 54 mg/L; see SM) suggesting possible occurrence of

381   DNAPL over most or nearly all of the contamination history. Based on site history, DNAPL contaminants

382   were disposed in the Southern Dump between the late 1950s and 1970s. Transport time was varied from

383   10 to 60 years to represent the possible time lapse between initial contamination and field characterization

384   in 2013. A best fit between modeled and measured profiles was obtained for 40 years of diffusive migration

385   (Fig. 8) suggesting contamination reached the interface shortly after the waste disposal occurred.

386   The TCE profile in the Lower Q1 aquitard has its peak concentration a few cm below the aquifer-aquitard

387   interface, showing back-diffusion from the Lower Q1 aquitard into the Upper A1 aquifer suggesting a

15

388 recent shift to a lower concentration at the boundary over the diffusion time period (Chapman and Parker

389 2005). Although both PCE and TCE were likely present as DNAPL at this interface, a faster decline of TCE

390 compared to PCE may be best explained by their original composition in the DNAPL and higher effective

391 solubility for TCE, causing a more rapid depletion in TCE at the boundary as a result. In the case of the TCE

392 modeling, the time for 1-D diffusive migration derived from the PCE best-fit time (i.e. 40 years) and the

393 concentration of TCE at the interface was used as the fitting or adjustment parameter. A best fit was

394 determined considering two steps of decreasing TCE at the boundary corresponding to 70 mg/L for the first

395 12 years and 10 mg/L for the remaining 28 years. The iterative modeling approach described above was

396 corroborated using the source history model developed by Adamson et al. (2015b) with the same boundary

397 concentrations (SM Fig. S4, S5). However, the assumption of a two-stage boundary condition over-

398 simplifies the possibility for strong initial gradients and TCE mass transfer (loss) from the DNAPL source

399 followed by a stage with low concentrations at the boundary and a concentration gradient reversal that

400 would attenuate strongly due to diffusion both in and out of the lower Q1 aquitard. As an alternative

401 scenario, the source history model "tool" was applied assuming an exponentially declining source (SM Fig.

402 S6), also providing a reasonable fit to the measured profile although with slightly larger associated error.

403 This shows the non-unique nature of fits for various assumptions regarding source history conditions.

404 Further to this, DNAPL invasion into the micro-fractures of the Lower Q1 cannot be completely ruled out.

405 Thus, the influence of a single fracture volume of DNAPL invading a typical size fracture in clays, assumed to

406 by 10-50 microns in aperture (e.g. Jørgensen et al. 1998, O'Hara et al. 2000, Hinsby et al. 1996, McKay et al.

407 1993, Jørgensen et al. 2002, Rudolph et al. 1991), was evaluated. The time of diffusion-based mass transfer

408 of PCE and TCE from DNAPL phase in the fractures causing complete DNAPL dissolution from the fractures

409 was estimated between 38 days and 2.6 years for PCE and between 1 and 32 days for TCE following Parker

410 et al. (1994) (details in the SM). Given such quick disappearance times by a single loading of DNAPL

411 invading these fractures with small apertures, possible dissolution of DNAPL by diffusion from the micro-

412 fractures would have unlikely interfered with the observed diffusion transport characteristics of the

413 profiles, as confirmed by the ability to simulate these PCE and TCE profiles . However, it is also unlikely that

16

414 a single fracture filling of DNAPL would occur after entry when DNAPL persists at the overlying aquifer-

415 aquitard interface, hence the simplest scenario of no DNAPL entry into the lower Q1 aquitard seems most

416 reasonable and defensible interpretation. Furthermore, it is also expected that DNAPL retention occurs

417 with depth of migration, causing lower volumes of DNAPL at the top of this lower Q1 aquitard interface,

418 making it difficult to overcome entry pressures in deep micro-fractures.

419

420 **5 Conclusions**

421 Three clay-rich non-indurated aquitards in a multi-layered aquifer-aquitard system of alluvial origin did not

422 prevent deep DNAPL migration to lower aquifers likely due to the occurrence of small-scale lithologic

423 heterogeneities and micro-fractures. This observation was made in a setting where, before this study, the

424 aquitards were considered protective of groundwater in the underlying aquifers based on standard

425 methods of site characterization such as lithology descriptions and bulk hydraulic conductivities. Whereas

426 the intermediate aquitard showed low integrity allowing fast advective migration of contaminants towards

427 the underlying aquifer due to occurrence of lithologic heterogeneities, the deepest aquitard showed

428 evidence of DNAPL accumulation at the upper boundary and only diffusive transport (i.e. diffusion profiles)

429 with sorption due to partitioning to solid phase organic carbon without discernable effects of advection,

430 suggesting much higher aquitard integrity. The high-resolution concentration profiles showed that the two

431 shallower aquitard units Q0 and Upper Q1 retained considerable DNAPL mass at/near their upper

432 boundaries and strongly reduced the flux of DNAPL to the lower system, but not completely preventing

433 deep migration. Both aquitards enhanced contaminant biodegradation due to high organic carbon content

434 influencing the contaminant mixtures that reached the underlying aquifers. At the core locations, it appears

435 that DNAPL did not enter the deepest Lower Q1 aquitard as diffusion transport matches the sharp

436 concentration decline with distance from the top of the aquitard over approximately 40 years. However,

437 deeper contamination in the Lower A1 aquifer, although at much lower concentrations, is observed most

438 likely due to some DNAPL penetration of the Lower Q1 aquitard up-gradient from the core locations or

439 aqueous phase transport along flow lines traveling through the DNAPL in the overlying units, making the

integrity assessment of the Lower Q1 aquitard uncertain beyond the local study area. Concentration

profiles produced by diffusive transport in this aquitard allowed assessing the approximate timing since

initial contaminant arrival at the top of the aquitard, which appears to have occurred with minimal delay

from surficial contamination events, suggesting rapid DNAPL migration through the subsurface. The two

deeper aquitards impeded DNAPL fluxes to some extent, with accumulation on these units fostering

diffusion into aquitards where substantial mass resides as dissolved and sorbed phases, posing a secondary,

long term source of contamination to the adjacent aquifers due to slow back-diffusion, even after complete

dissolution of the DNAPL or active remediation of the waste zone. Knowing that preferential accumulation

occurred at the top of lower K clay-rich units should also guide placement of future monitoring points. The

different behavior observed for distinct aquitards of the same multi-layer aquifer-aquitard system

highlights the need for high-resolution aquitard-specific investigations for (1) defining the degree of

protection provided to the underlying aquifers, and (2) assessing the long-term influence that aquitards

might have on contaminant phase re-distribution and transformation. Follow-on studies might enhance the

vertical high-resolution information in the lateral directions e.g. by exploring the lateral continuity and

geometry of the aquitard-aquifer interfaces by means of lower invasive technologies such as geophysics.

References

Adamson, D.T., Chapman, S.W., Farhat, S.K., Parker, B.L., deBlanc, P., Newell, C.J., 2015a. Characterization

and Source History Modeling Using Low-k Zone Profiles at Two Source Areas. Groundwater Monitoring &

Remediation: n/a-n/a.

466   Adamson, D.T., Chapman, S.W., Farhat, S.K., Parker, B.L., deBlanc, P.C., Newell, C.J., 2015b. Simple

467   Modeling Tool for Reconstructing Source History Using High Resolution Contaminant Profiles From Low-k

468   Zones. Remediation Journal, 25(3): 31-51.

469   Amorosi, A., Centineo, M.C., Dinelli, E., Lucchini, F., Tateo, F., 2002. Geochemical and mineralogical

470   variations as indicators of provenance changes in Late Quaternary deposits of SE Po Plain. Sedimentary

471   Geology, 151(3–4): 273-292.

472   Amorosi, A., Colalongo, M.L., 2005. The Linkage between Alluvial and Coeval Nearshore Marine

473   Successions: Evidence from the Late Quaternary Record of the PO River Plain, Italy, Fluvial Sedimentology

474   VII. Blackwell Publishing Ltd., pp. 255-275.

475   Amorosi, A., Marchi, N., 1999. High-resolution sequence stratigraphy from piezocone tests: an example

476   from the Late Quaternary deposits of the southeastern Po Plain. Sedimentary Geology, 128(1–2): 67-81.

477   Blum, M.D., Törnqvist, T.E., 2000. Fluvial responses to climate and sea-level change: a review and look

478   forward. Sedimentology, 47: 2-48.

479   Carslaw, H.S., Jaeger, J.C., 1959. Conduction of heat in solids (2nd Ed.). Clarendon Press, Oxford.

480   Chapman, S.W., Parker, B.L., 2005. Plume persistence due to aquitard back diffusion following dense

481   nonaqueous phase liquid source removal or isolation. Water Resources Research, 41(12): W12411.

482   Chapuis, R.P., 2013. Contamination of till aquitard by DNAPL: is it actual, or drilling artefact? . Geotechnical

483   News, 31(4): 36-38.

484   Chen, B.S., Mayne, P.W., 1996. Statistical relationships between piezocone measurements and stress

485   history of clays. Canadian Geotechnical Journal, 33(3): 488-498.

486   Cherry, J.A., Parker, B.L., Bradbury, K.R., Eaton, T.T., Gotkowitz, M.G., Hart, D.J., Borchardt, M.A., 2006.

487   Contaminant Transport Through Aquitards: A "State of the Science" Review, AWWA Research Foundation,

488   Denver, Colorado.

489   Dincutoiu, I., Górecki, T., Parker, B.L., 2003. A Novel Technique for Rapid Extraction of Volatile

490   Organohalogen Compounds from Low Permeability Media. Environmental Science & Technology, 37(17):

491   3978-3984.

492   Einarson, M.D., 2006. Multilevel Ground-water Monitoring. In: D.M. Nielson (Editor), Practical Handbook of

493   Environmental Site Characterization and Ground-Water Monitoring, 2nd ed. CRC Press, Boca Raton, FL,

494   USA, pp. 807-848.

495   Einarson, M.D., Cherry, J.A., 2002. A New Multilevel Ground Water Monitoring System Using Multichannel

496   Tubing. Ground Water Monitoring & Remediation, 22(4): 52-65.

497   Filippini, M., Amorosi, A., Campo, B., Herrero-Martìn, S., Nijenhuis, I., Parker, B.L. and Gargini, A., 2016.

498   Origin of VC-only plumes from naturally enhanced dechlorination in a peat-rich hydrogeologic setting.

499   Journal of Contaminant Hydrology, 192: 129-139.

500   Filippini, M., Stumpp, C., Nijenhuis, I., Richnow, H.H., Gargini, A., 2015. Evaluation of aquifer recharge and

501   vulnerability in an alluvial lowland using environmental tracers. Journal of Hydrology, 529, Part 3: 1657-

502   1668.

503   Fjordbøge, A.S., Janniche, G.S., Jørgensen, T.H., Grosen, B., Wealthall, G., Christensen, A.G.,

504   Kerrn-Jespersen, H., Broholm, M.M., 2017. Integrity of Clay Till Aquitards to DNAPL Migration: Assessment

505   Using Current and Emerging Characterization Tools. Groundwater Monitoring & Remediation, 37(3): 45-61.

506   Gargini, A., Pasini, M., Picone, S., Rijnaarts, H., Van Gaans, P., 2011. Chlorinated hydrocarbons plumes in a

507   residential area. Site investigation to assess indoor vapor intrusion and human health risks. In: S. Saponaro,

508   E. Sezenna, L. Bonomo (Editors), Vapor emission to outdoor air and enclosed spaces for human health risk

509   assessment: site dharacterization, monitoring and modelling. Nova Science Publishers, Inc., Milan, Italy, pp.

510   211-233.

511   Green, W.J., Lee, G.F., Jones, R.A., 1981. Clay-Soils Permeability and Hazardous Waste Storage. Water

512   Pollution Control Federation, 54(8): 1347-1354.

513   Hinsby, K., McKay, L.D., JØrgensen, P., Lenczewski, M., Gerba, C.P., 1996. Fracture Aperture Measurements

514   and Migration of Solutes, Viruses, and Immiscible Creosote in a Column of Clay-Rich Till. Ground Water,

515   34(6): 1065-1075.

516 Jørgensen, P.R., Hoffmann, M., Kistrup, J.P., Bryde, C., Bossi, R., Villholth, K.G., 2002. Preferential flow and

517 pesticide transport in a clay-rich till: Field, laboratory, and modeling analysis. Water Resources Research,

518 38(11): 28-1-28-15.

519 Jørgensen, P.R., McKay, L.D., Spliid, N.H., 1998. Evaluation of chloride and pesticide transport in a fractured

520 clayey till using large undisturbed columns and numerical modeling. Water Resources Research, 34(4): 539-

521 553.

522 Kueper, B.H., McWhorter, D.B., 1991. The Behavior of Dense, Nonaqueous Phase Liquids in Fractured Clay

523 and Rock. Ground Water, 29(5): 716-728.

524 Legates, D.R., McCabe Jr, G.J., 1999. Evaluating the use of "goodness-of-fit" measures in hydrologic and

525 hydroclimatic model validation. Water resources research, 35(1): 233-241.

526 Mayne, P.W., Kulhawy, F.H., Kay, J.N., 1990. Observations on the development of pore-water stresses

527 during piezocone penetration in clays. Canadian Geotechnical Journal, 27(4): 418-428.

528 McKay, L.D., Cherry, J.A., Gillham, R.W., 1993. Field experiments in a fractured clay till: 1. Hydraulic

529 conductivity and fracture aperture. Water Resources Research, 29(4): 1149-1162.

530 McWhorter, D., Kueper, B., 1996. Mechanics and mathematics of the movement of dense non-aqueous

531 phase liquids (DNAPLs) in porous media. Dense Chlorinated Solvents and Other DNAPLs in Groundwater;

532 History, Behavior, and Remediation: 89-128.

533 Mitra, S., Prakash, D., 1956. Adsorption of potassium as influenced by concentration and pH of the solution.

534 Clay Miner, 3: 151-153.

535 Molinari, F.C., Boldrini, G., Severi, P., Dugoni, G., Rapti Caputo, D., Martinelli, G., 2007. Risorse idriche

536 sotterranee della Provincia di Ferrara (in italian; transl. Groundwater resources of the Ferrara Province),

537 Risorse idriche sotterranee della Provincia di Ferrara (in italian; transl. Groundwater resources of the

538 Ferrara Province). DB-MAP printer, Florence, Italy, pp. 1-62.

539 Morrison, W.E., Parker, B.L., Cherry, J.A., 1998. Hydrogeological controls on flow and fate of PCE DNAPL in a

540 fractured and layered clayey aquitard: a Borden experiment, Geological Society of America, annual

541 meeting. Geological Society of America, Boulder, CO.

542 Narasimhan, T.N., 2004. Fick's insights on liquid diffusion. Eos, Transactions American Geophysical Union,

543 85(47): 499-501.

544 Nash, J.E., Sutcliffe, J.V., 1970. River flow forecasting through conceptual models part I — A discussion of

545 principles. Journal of Hydrology, 10(3): 282-290.

546 Ndon, U.J., Randall, A.A., Khouri, T.Z., 2000. Reductive Dechlorination of Tetrachloroethylene by Soil

547 Sulfate-Reducing Microbes under Various Electron Donor Conditions. Environmental Monitoring and

548 Assessment, 60(3): 329-336.

549 O'Hara, S.K., Parker, B.L., Jørgensen, P.R., Cherry, J.A., 2000. Trichloroethene DNAPL flow and mass

550 distribution in naturally fractured clay: Evidence of aperture variability. Water Resources Research, 36(1):

551 135-147.

552 Parker, B.L., 1996. Effects of Molecular Diffusion on the Persistence of Dense Immiscible Organic Liquids in

553 Fractured Porous Media. Ph.D. diss. University of Waterloo, Waterloo, Ontario.

554 Parker, B.L., Cherry, J.A., Chapman, S.W., 2004. Field study of TCE diffusion profiles below DNAPL to assess

555 aquitard integrity. Journal of Contaminant Hydrology, 74(1–4): 197-230.

556 Parker, B.L., Cherry, J.A., Chapman, S.W., Guilbeault, M.A., 2003. Review and analysis of chlorinated solvent

557 DNAPL distributions in five sandy aquifers. Vadose Zone J 2: 116-137.

558 Parker, B.L., Gillham, R.W., Cherry, J.A., 1994. Diffusive Disappearance of Immiscible-Phase Organic Liquids

559 in Fractured Geologic Media. Ground Water, 32(5): 805-820.

560 Pedretti, D., Masetti, M., Beretta, G.P., Vitiello, M., 2013. A Revised Conceptual Model to Reproduce the

561 Distribution of Chlorinated Solvents in the Rho Aquifer (Italy). Groundwater Monitoring & Remediation,

562 33(3): 69-77.

563 Pickering, W.F., 1985. The mobility of soluble fluoride in soils. Environmental Pollution Series B, Chemical

564 and Physical, 9(4): 281-308.

565 Ponzini, G., Crosta, G., Giudici, M., 1989. The hydrogeological role of an aquitard in preventing drinkable

566 water well contamination: a case study. Environmental Health Perspectives, 83: 77-95.

567 PPG Industries, 1995. Phase 2, Draft Site Wide RCRA Facility Investigation, U.S. EPA.

568   Rapti-Caputo, D., Martinelli, G., 2009. The geochemical and isotopic composition of aquifer systems in the

569   deltaic region of the Po River plain (northern Italy). Hydrogeology Journal, 17(2): 467-480.

570   Regione Emilia-Romagna, ENI-AGIP, 1998. Riserve idriche sotterranee della Regione Emilia-Romagna (In

571   italian; transl.: Groundwater resources of the Emilia-Romagna Region). S.EL.CA. printer, Florence.

572   Rizzini, A., 1974. Holocene sedimentary cycle and heavy-mineral distribution, Romagna-Marche coastal

573   plain, Italy. Sedimentary Geology, 11(1): 17-37.

574   Rudolph, D.L., Cherry, J.A., Farvolden, R.N., 1991. Groundwater Flow and Solute Transport in Fractured

575   Lacustrine Clay Near Mexico City. Water Resources Research, 27(9): 2187-2201.

576   U.S. EPA, 1987. Guidelines for Delineation of Wellhead Protection Areas U.S. Environmental Protection

577   Agency, Office of Ground-Water Protection., Washington D.C.

578   U.S. EPA, 2003. Method 5030C, "Purge-and-trap for aqueous samples", U.S. Environmental Protection

579   Agency.

580   U.S. EPA, 2006. Method 8260C "Volatile Organic Compounds By Gas Chromatography/Mass Spectrometry

581   (GC/MS)", U.S. Environmental Protection Agency.

582   Wanner, P., Parker, B., Chapman, S.W., Aravena, R., Hunkeler, D., 2016. Quantification of Degradation of

583   Chlorinated Hydrocarbons in Saturated Low Permeability Sediments Using Compound-Specific Isotope

584   Analysis (CSIA). Environmental science & technology.

585   Wills, J., Howell, L., McKay, L., Parker, B.L., Walter, A., 1992. Smithville C.W.M.L. Site: Characterizations of

586   overburden fractures and implications for DNAPL Transport, Modern Trends in Hydrogeology- IAH Canadian

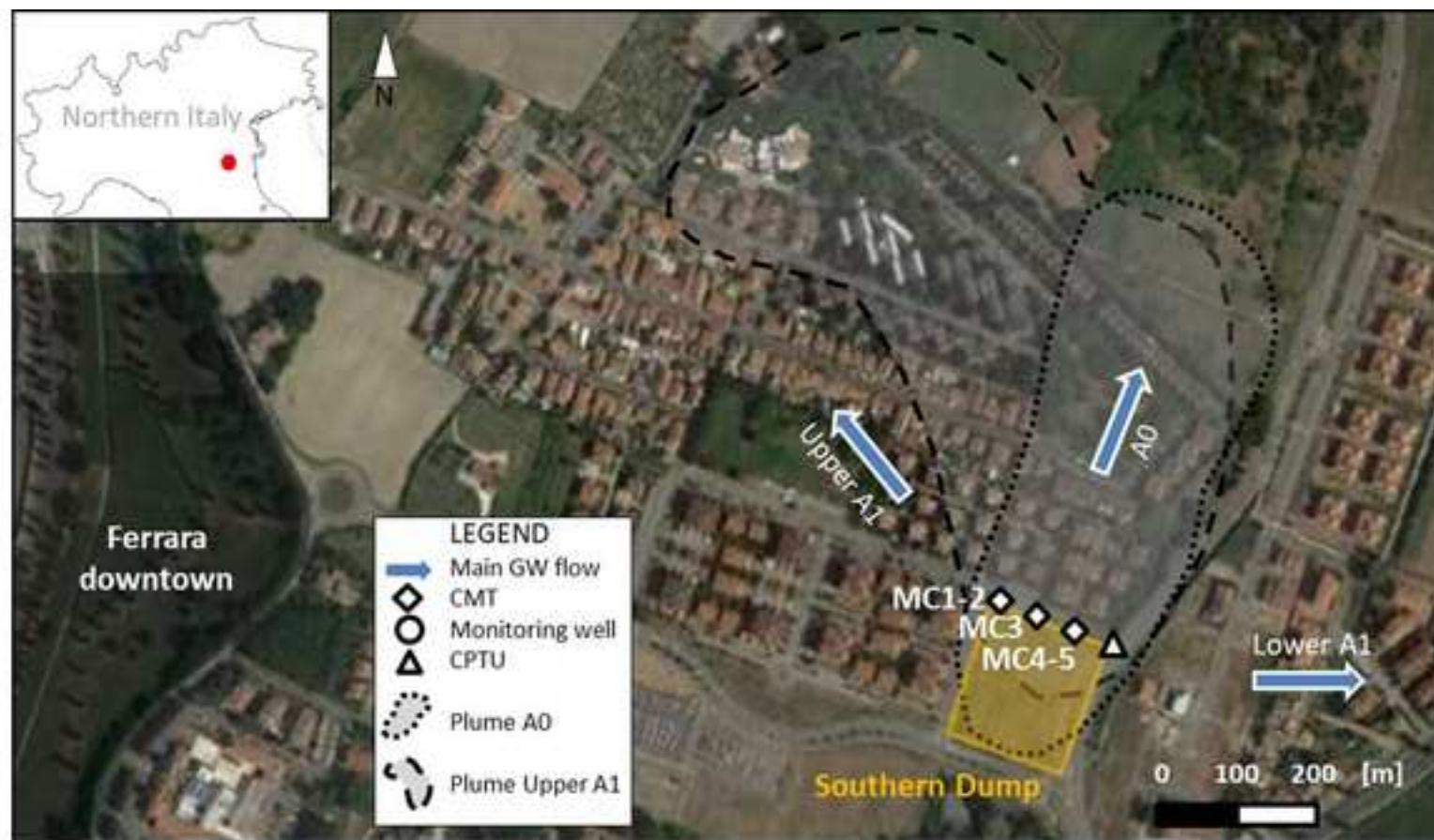587   Chapter Conference, Hamilton, Ontario, pp. 501-515.

588

589

Figure 1: Monitoring network at the Caretti site. The CMT transect ("MC1-2", "MC3", "MC4-5" systems), disposed on an edge of the Southern Dump, is described in detail in Fig. 2. The location of a Cone Penetration Test (CPTU) performed close to the CMT transect is reported on the map (see CPTU results in Fig. 4). The main groundwater flow directions and the mixed contaminant plumes were outlined based on data from Nijenhuis et al. (2013) and Gargini et al. (2011).

Figure2
Click here to download high resolution image
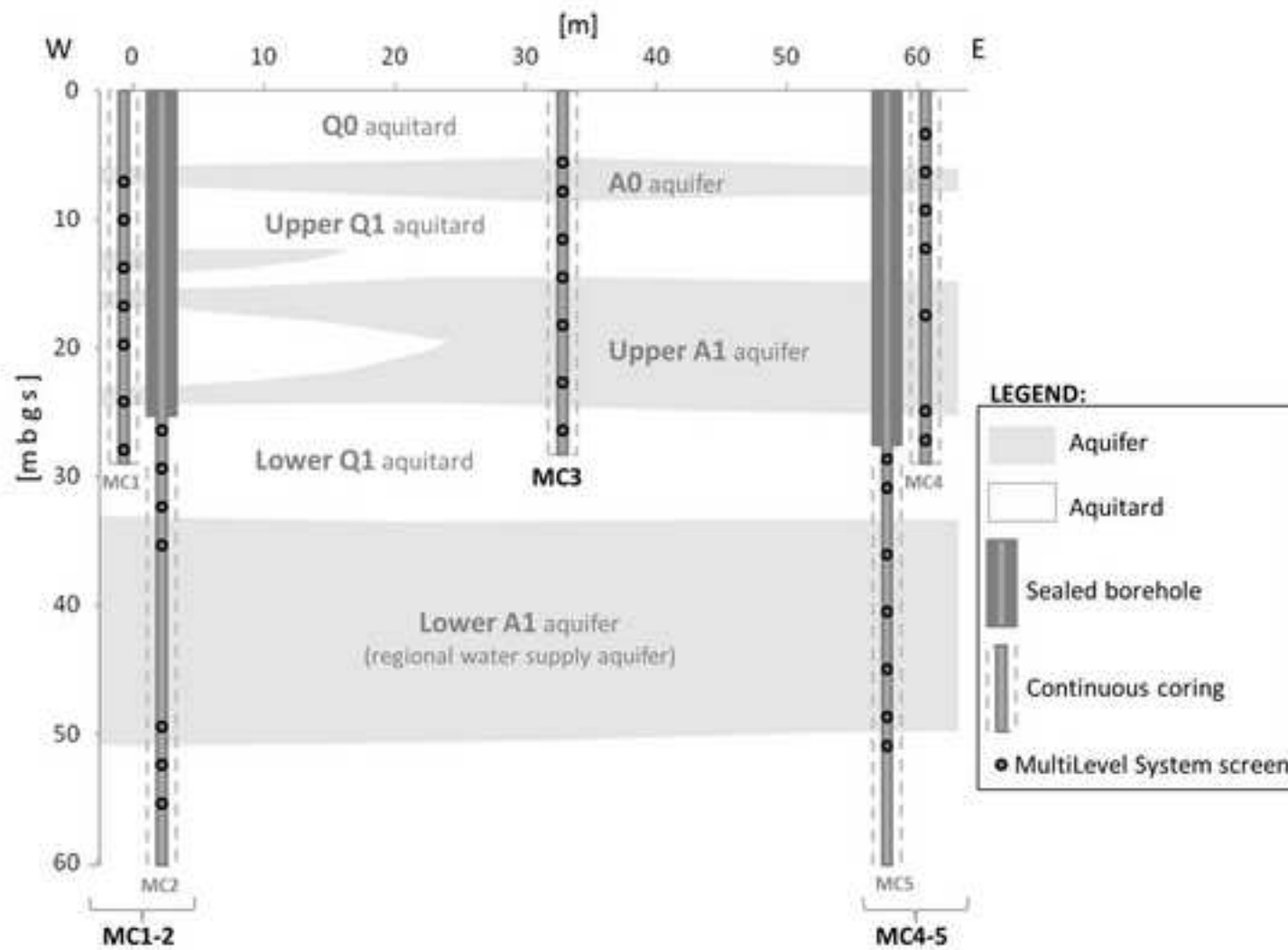
Figure2: Schematic of the CMT transect (see location of the cross-section in Fig. 1). Detailed stratigraphic logs of cores MC1-2, MC3 and MC4-5 are shown in Fig. 3.

Figure3
Click here to download high resolution image
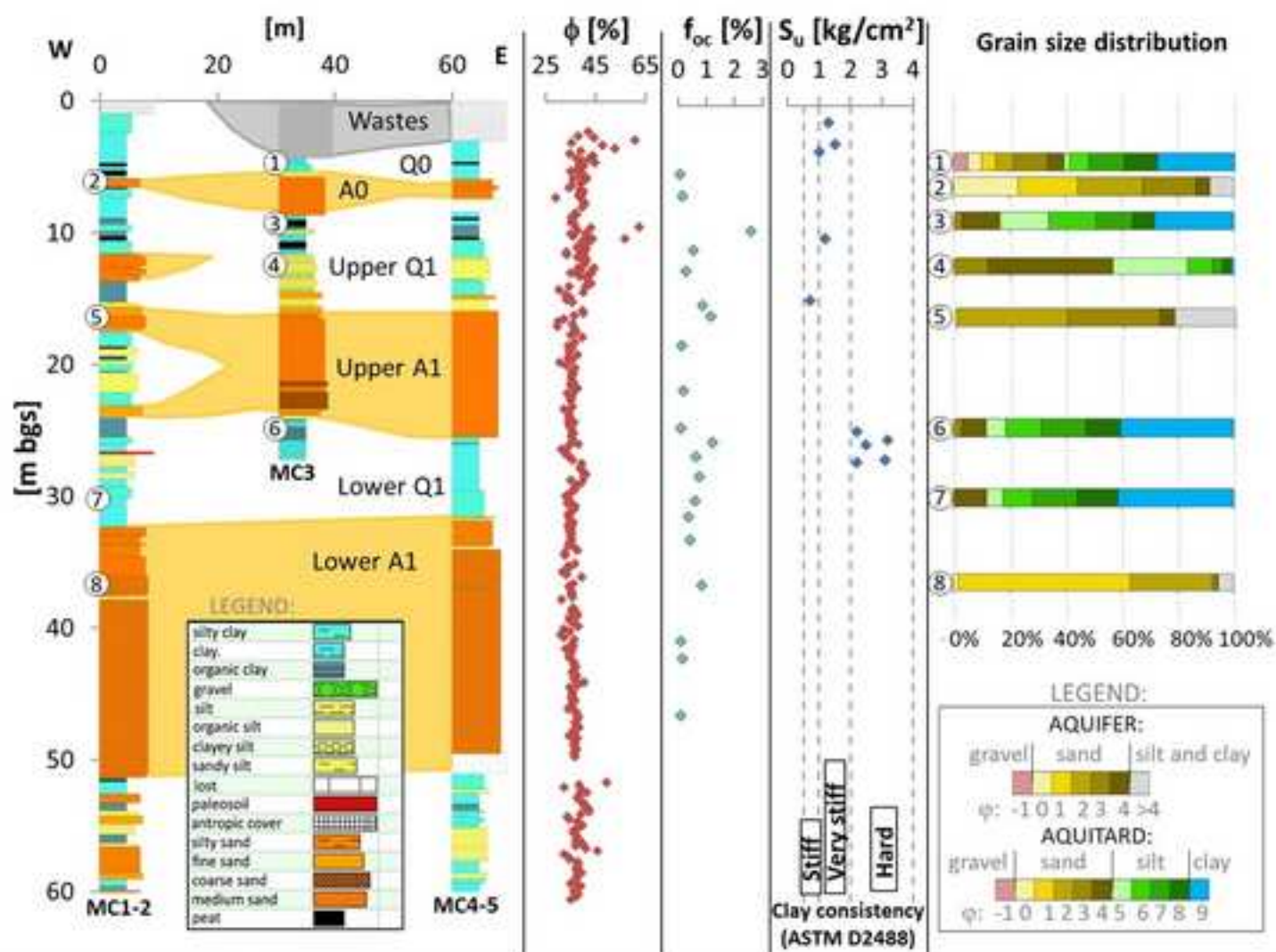
Figure 3: Stratigraphic information collected along the transect. From the left: geologic logs and geometry of aquifers and aquitards; vertical trend of estimated total porosity (ϕ; from profile MC4-5); vertical trend of organic carbon content (f_{oc}; from core MC4-5); estimations of undrained cohesion (S_u) on clayey layers via pocket penetrometer tests (from core MC1-2); grain size distribution of aquifers and aquitards (sampling depths indicated with numbers on the MC1-2 and MC3 geologic logs).

Figure 4: Vertical distribution of chloroethenes (a), chloroethanes (b) and chloromethanes (c). From left: concentrations from groundwater samples (GW; Log mg/L - only concentrations >0.1 mg/L are plotted for graphical reasons (black crosses indicate GW samples with concentration < 0.1 mg/L for all the analyzed compounds); total concentrations in sediment samples along profile MC4-5 (Ct, Log μg/g – only concentrations > 0.1 μg/g are plotted for graphical reasons); estimated pore water concentrations from phase partitioning (Cw; Log mg/L –- only concentrations > 0.1 mg/L are plotted for graphical reasons); estimated sorbed mass concentrations from phase partitioning (Cs; Log μg/g – only concentrations > 0.1 μg/g are plotted for graphical reasons). The one sample with estimated pore water concentration of PCE most likely higher than effective solubility is highlighted with a black arrow. The concentration database is in Tables S2 and S3 of the SM.

Figure5
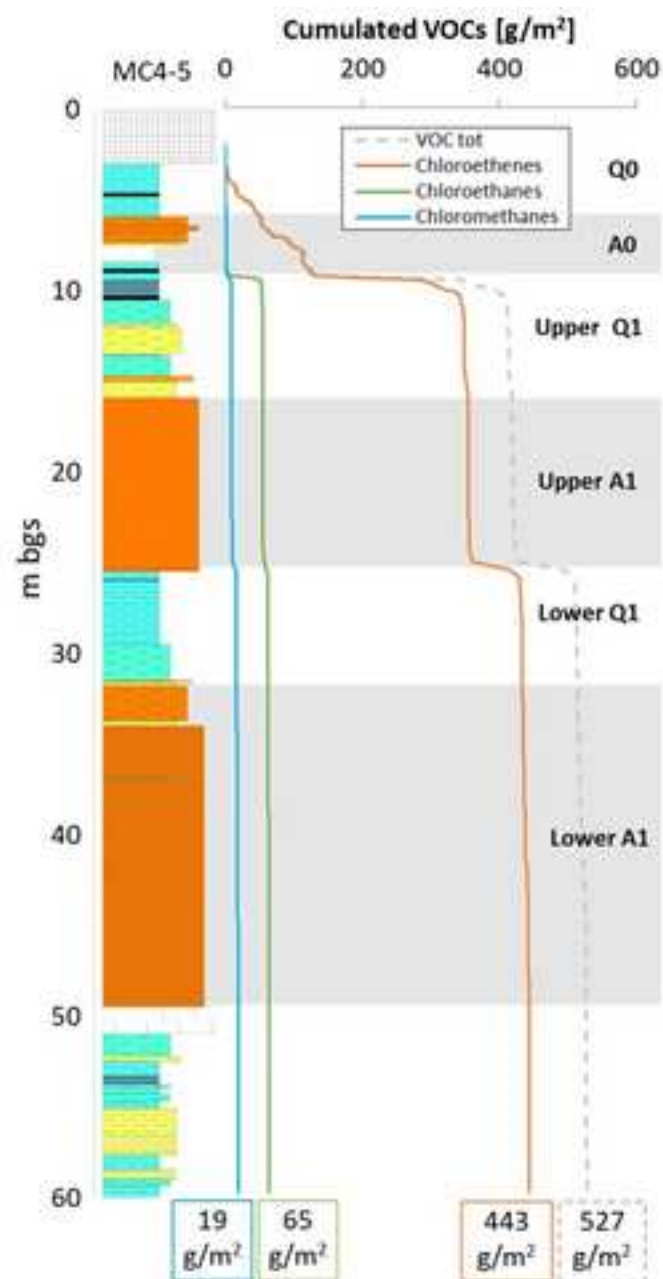**Click here to download high resolution image**

Figure 5: Profiles of cumulative mass per unit area of total VOC, chloroethenes, chloroethanes and chloromethanes at MC4-5 location. Calculations of cumulative mass per unit area are described in the SM.
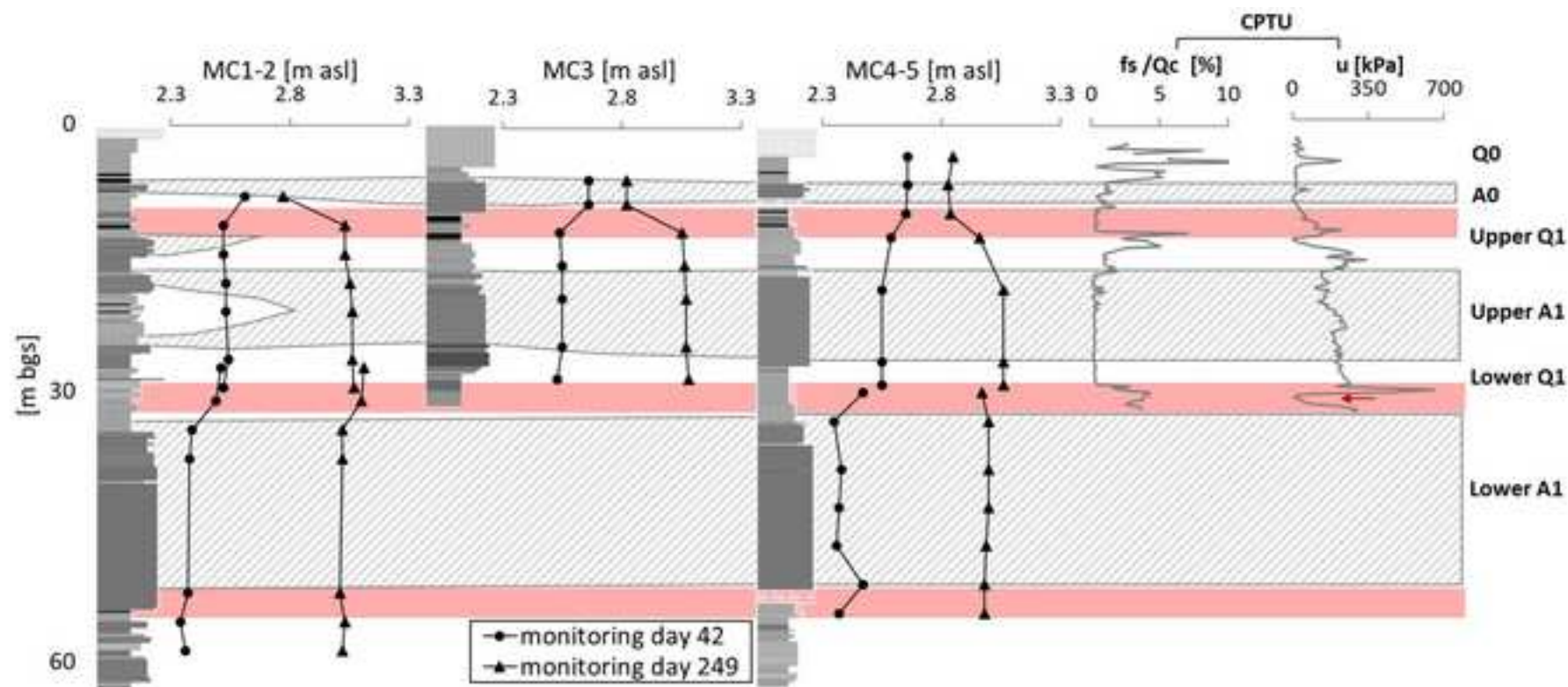
Figure6
Click here to download high resolution image

Figure 6: Vertical head distribution along the three profiles of the transect at monitoring days n. 42 and 249. The pink stripes indicate the sections with the steepest hydraulic vertical gradient within in the aquitards. The results of a CPTU test performed 50 m southeastward from the transect are reported beside the head profiles (see CPTU location in Fig. 1). The red arrow highlights a significant decrease of pore pressure (u) that occurs around 30 m bgs in correspondence of the steepest hydraulic vertical gradient in the lower Q1 aquitard.

Figure7
Click here to download high resolution image
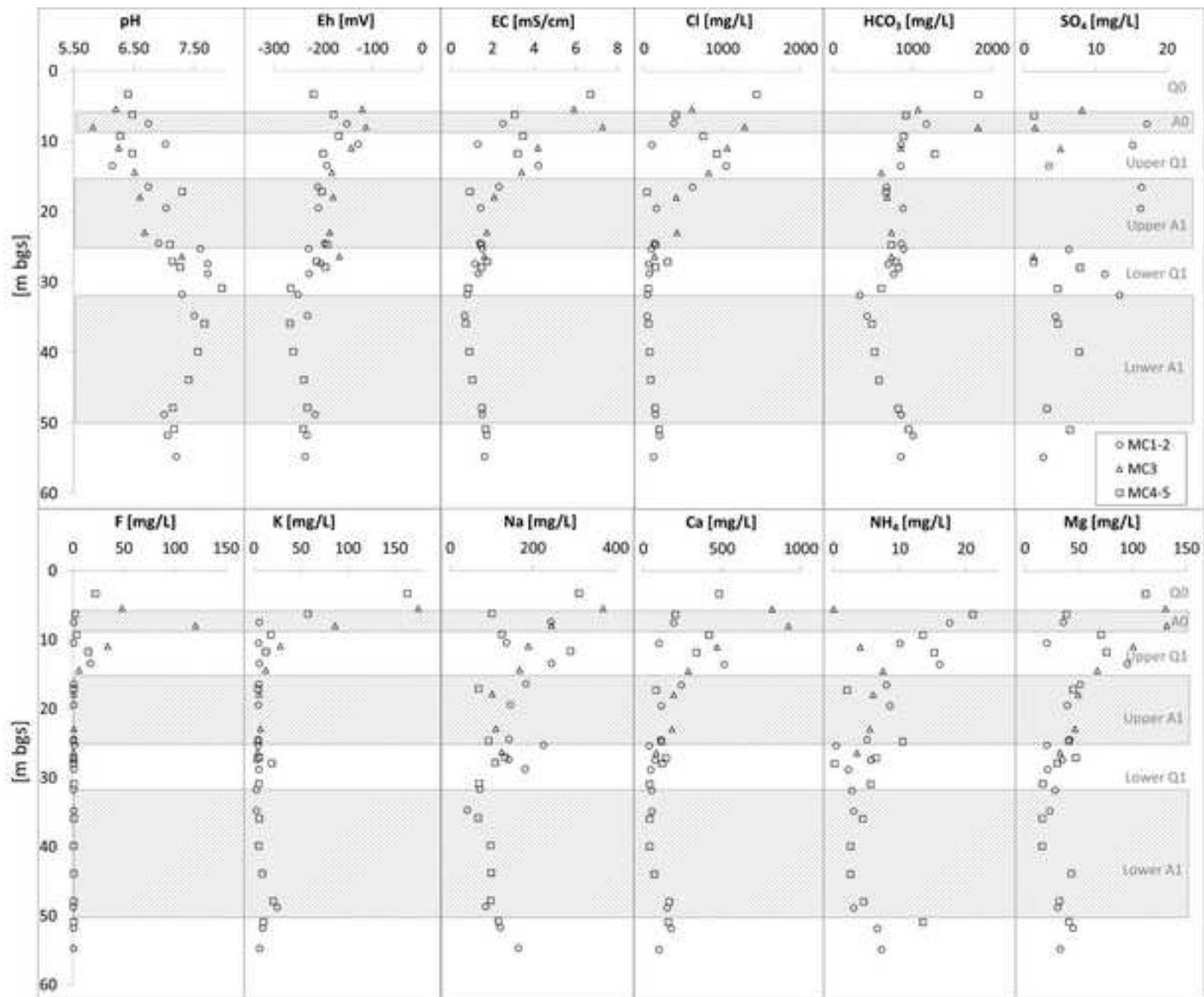
Figure 7: Vertical trends of the main chemical parameters of groundwater and dissolved ions along the three profiles of the transect.
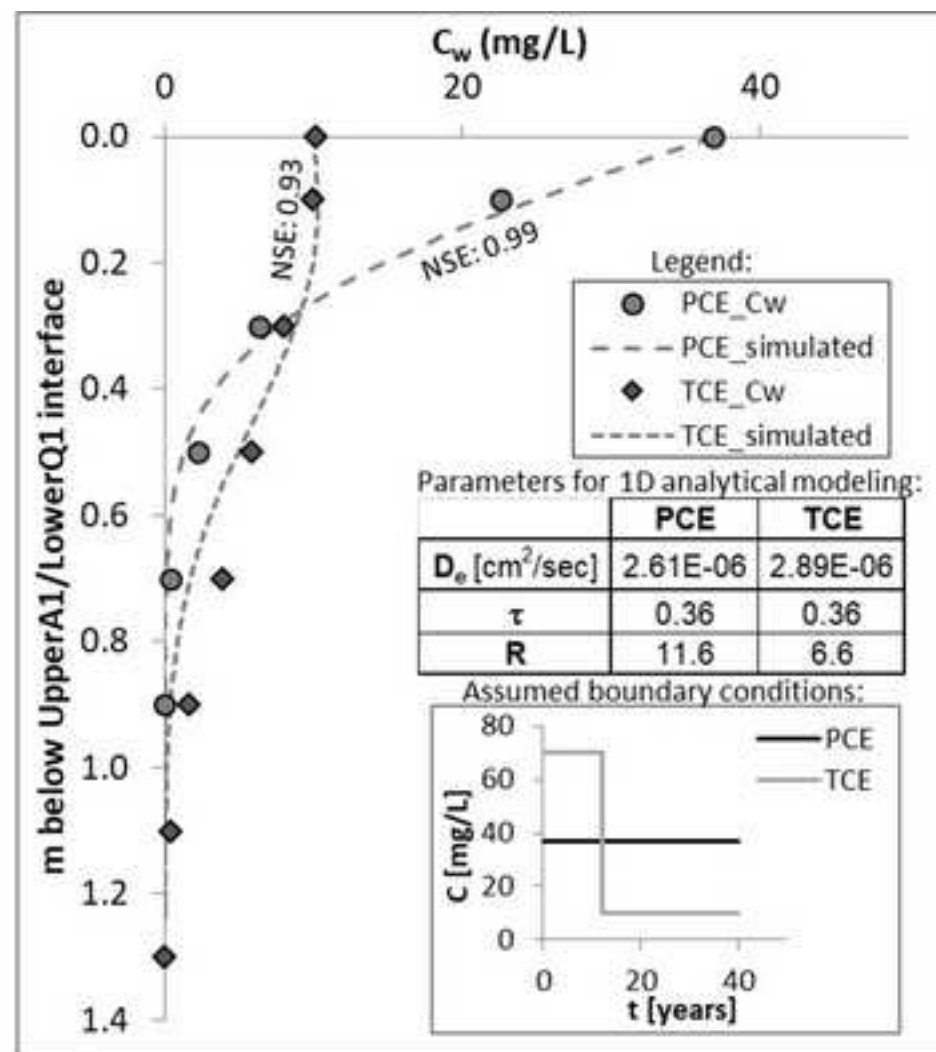
Figure 8: Results of 1D analytical simulation of diffusion profiles of PCE and TCE. The goodness of fit with measured Cw data is reported based on Nash–Sutcliffe model efficiency coefficient (NSE).

Field parameters and contaminant concentrations